ACS NANO
Cite This: ACS Nano XXXX, XXX, XXX−XXX
www.acsnano.org

ARTICLE

Single-Droplet Multiplex Bioassay on a Robust and Stretchable Extreme Wetting Substrate through Vacuum-Based Droplet Manipulation

Heetak Han,[†] Jung Seung Lee,[‡] Hyunchul Kim,[†] Sera Shin,[†] Jaehong Lee,[†] Jongchan Kim,[§] Xu Hou,[⊥] Seung-Woo Cho,[‡] Jungmok Seo,*[,∥,#] and Taeyoon Lee*[,†]

[†]School of Electrical and Electronic Engineering and [‡]Department of Biotechnology, Yonsei University, Seoul, 03722, Republic of Korea

[§]Department of Electrical Engineering and Computer Science, University of Michigan, Ann Arbor, Michigan 48109, United States

[⊥]College of Chemistry and Chemical Engineering, Collaborative Innovation Center of Chemistry for Energy Materials, and State Key Laboratory of Physical Chemistry of Solid Surfaces, Xiamen University, Xiamen 361005, China

[∥]Center for Biomaterials, Biomedical Research Institute, Korea Institute of Science and Technology (KIST), Seoul 02792, Republic of Korea

[#]Division of Bio-Medical Science & Technology, KIST School, Korea University of Science and Technology (UST), Seoul 02792, Republic of Korea

Supporting Information

ABSTRACT: **Herein, a droplet manipulation system with a superamphiphobic (SPO)−superamphiphilic (SPI) patterned polydimethylsiloxane (PDMS) substrate is developed for a multiplex bioassay from single-droplet samples. The SPO substrate is fabricated by sequential spraying of adhesive and fluorinated silica nanoparticles onto a PDMS substrate. It is subsequently subjected to oxygen plasma with a patterned mask to form SPI patterns. The SPO layer exhibits extreme liquid repellency with a high contact angle (>150°) toward low surface tension and viscous biofluidic droplets (*e.g.*, ethylene glycol, blood, dimethyl sulfoxide, and alginate hydrogel). In contrast, the SPI exhibits liquid adhesion with a near zero contact angle. Using the droplet manipulation system, various liquid droplets can be precisely manipulated and dispensed onto the predefined SPI patterns on the SPO PDMS substrate. This system enables a multiplex colorimetric bioassay, capable of detecting multiple analytes, including glucose, uric acid, and lactate, from a single sample droplet. In addition, the detection of glucose concentrations in a plasma droplet of diabetic and healthy mice are performed to demonstrate the feasibility of the proposed system for efficient clinical diagnostic applications.**

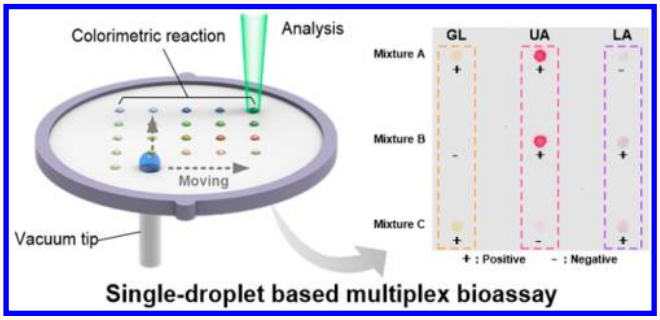

KEYWORDS: *superamphiphobic, bioassay, droplet manipulation, colorimetric analysis, biomimetics*

Droplet-based microfluidic systems have received significant attention because they enable efficient biological and chemical analyses with a small sample amount and simple reagents.[1−3] Compared to conventional microfluidic devices with fluidic channels, droplet-based microfluidic systems provide greater flexibility and versatility because they do not require complex channel networks, pumps, or tubing systems.[4] Several approaches can be used to control droplet samples on a substrate using surface energy gradients,[5] electrowetting,[6] electromagnetic force,[7−10] light,[11,12] and acoustic wave.[13] However, these methods often require additives, such as electrolytes or magnetizable particles, to enhance the response of liquid droplets to applied forces, which hinders the use of droplet-based microfluidic systems for many analytical applications.[9,14]

Extremely water-repellent superhydrophobic surfaces have attracted significant interest for use in droplet-based microfluidics because they enable facile droplet manipulation without the use of additives.[15−17] However, the full-range of manipulations of water droplets, such as transporting, mixing, and dispensing, has rarely been demonstrated on a superhydrophobic surface because of the lack of facile droplet manipulation methods.

Received: August 16, 2017
Accepted: December 20, 2017
Published: December 20, 2017

DOI: 10.1021/acsnano.7b05826
ACS Nano XXXX, XXX, XXX−XXX

Electrowetting is widely used in droplet-based microfluidic systems because of its capability for comprehensive droplet manipulation.[6,9] Although electrowetting allows facile droplet manipulation, it requires a closed system with high applied voltage, which restricts its versatility for various biological applications. Therefore, the development of a droplet manipulation system using a superhydrophobic surface is urgently needed.

Recently, we developed a droplet-based microfluidic platform that enabled the full-range of manipulations of individual water droplets through reversible local deformation of microstructured superhydrophobic substrates.[18] Although the developed droplet-based microfluidic platform provided a high degree of freedom for droplet manipulation, it was not able to dispense small amounts of liquid from the sample. To the best of our knowledge, no droplet-based microfluidic system has been developed that allows full-range manipulation of low surface tension and viscous biofluidic droplets. The lack of an effective manipulation method for droplet samples limits the applications of related multiplex bioassays and point-of-care diagnostics.

Analysis of biological analytes in human bodily fluids is required for the diagnosis and management of chronic diseases.[19−21] Various biosensing techniques, including fluorescence,[22,23] electrochemistry,[24,25] chemiluminescence,[26,27] biobarcode assays,[28,29] and colorimetric bioassays,[30,31] have been developed to detect/measure biological analytes. Among these methods, colorimetric bioassays have attracted particular attention because of their straightforward, rapid, and easily recognizable response without the need for expensive or sophisticated instruments. The combination of a colorimetric bioassay and a droplet-based microfluidic platform would likely prove to be beneficial for the development of point-of-care devices that enable multiplex bioassays using a single droplet.[20,32−34]

Herein, we report a strategy that enables full-range manipulation of various liquid droplets, including water, ethylene glycol (EG), blood, dimethyl sulfoxide (DMSO), and hydrogels. A stretchable superamphiphobic (SPO)−superamphiphilic (SPI) patterned polydimethylsiloxane (PDMS) substrate was the platform with which we were able to achieve the full-range manipulation. The SPO layer was fabricated through sequential spray coating of a double layer of adhesive and fluorinated silica nanoparticles (F-NPs) on a thin and flexible PDMS substrate. The SPO-layer-coated PDMS (SPO PDMS) substrate exhibited extremely high liquid repellency with a large contact angle (CA) of >150° and a low sliding angle (SA) of <10° toward various liquid droplets. The surface maintained its superamphiphobicity even under high strain rates (>100%) and repeated stretching cycles (>1000 cycles). To manipulate a liquid droplet on the substrate, a local dimple structure was formed by placing a moving vacuum tip under the substrate. Liquid droplets in the SPO region were easily moved along the local dimple structure because of the extremely low surface adhesion force. To form SPI patterns on the SPO PDMS substrate, the substrate was treated with oxygen plasma and a shadow mask. After defining the SPI regions on the SPO PDMS substrate, liquid droplets with a volume of 0.05−1.4 μL were precisely dispensed onto the SPI patterns through the fabricated droplet manipulation system. Thus, a single-droplet multiplex colorimetric bioassay was demonstrated. Various biological analytes such as glucose (GL), uric acid (UA), and lactate (LA) over clinically relevant ranges (GL, 0−20 mM; UA, 0.25−4 mM; LA, 0−20 mM) were successfully analyzed using the developed system. In addition, diabetes diagnoses were conducted by determination of the GL concentrations in the plasma of healthy and diabetic mice.

RESULTS AND DISCUSSION

Fabrication of SPO−SPI Patterned PDMS Substrate for a Single-Droplet Multiplex Colorimetric Bioassay Platform. Figure 1a shows a schematic of the single-droplet multiplex colorimetric bioassay platform. A predesigned colorimetric bioassay library is formed on the SPO−SPI patterned PDMS substrate as a disposable cartridge. Upon loading the cartridge onto the droplet manipulation system, a single-droplet sample (*e.g.*, blood, tears, or urine) containing multiple biological analytes can be precisely manipulated by the local dimple structure generated by the application of a vacuum tip beneath the substrate. The droplet can easily be moved along the vacuum tip, and a very small volume of liquid can be dispensed onto each SPI pattern. The SPI patterns were predesigned with different colorimetric reagents to enable the examination of multiple analytes in the single-droplet sample.

Figure 1b shows the fabrication process of the SPO−SPI patterned PDMS substrate. First, the SPO layer is coated onto a thin and flat PDMS substrate using a simple and sequential spray of adhesive material and F-NPs. The SPI regions are then defined on the SPO layer by oxygen plasma treatment with a shadow mask. This enables the simple and large-area coating of the SPO layer with SPI patterns on various materials (see Figures S1 and S2 for more information). Figure 1c shows representative scanning electron microscopy (SEM) images of the fabricated SPO PDMS substrate. The SEM images show hierarchical micro- and nanostructures composed of bonding material and F-NPs deposited by spray coating. The generated micro/nanohierarchical structures maintained their morphology even after the oxygen plasma treatment (Figure S3).

The chemical composition of the SPO layer coated on the Si surface with and without plasma treatment was characterized by X-ray photoelectron spectroscopy (XPS), as shown in Figure 1d. The SPO layer spectrum shows a relatively large F 1s peak (689.4 eV) arising from the fluoroalkyl silane (FAS) of the F-NPs on the substrate.[35] The FAS was decomposed by reactive oxygen atoms from the plasma treatment, resulting in a decreased F 1s peak intensity in the XPS spectrum of the SPI substrate.[15] The SPO PDMS substrate exhibited extremely high liquid repellency for water, EG, blood, DMSO, and hydrogels. In contrast, the SPI surface exhibited extremely high liquid wettability, as shown in Figure 1e.

Extreme Wettability of the SPO and SPI PDMS Substrates. To characterize the wettability of the SPO/SPI coating layers, 10 μL blood samples were dropped onto 20°-tilted bare, SPO PMDS, and SPI-layer-coated PDMS (SPI PDMS) substrates (Figure 2a and Movie S1). In this study, 0.75 U/mL of heparin was used to prevent the immediate clotting of fresh blood droplets upon exposure to air.[36] When the blood sample was dropped onto a bare PDMS substrate, it adhered to the substrate and did not roll off. However, when it was dropped onto the SPO PDMS substrate, the blood droplet quickly rolled off due to gravitational forces, without leaving blood residue on the substrate. After plasma treatment, the wettability of the SPO surface dramatically changed, resulting in rapid spreading of the blood droplet on the substrate.

For quantitative analysis of the liquid wetting behaviors on the SPO/SPI substrates, the static CAs of the various types of droplets on SPO/SPI PDMS were measured (Figure 2b,c). All liquids used in this experiment showed a high CA (>150°)

DOI: 10.1021/acsnano.7b05826
ACS Nano XXXX, XXX, XXX−XXX

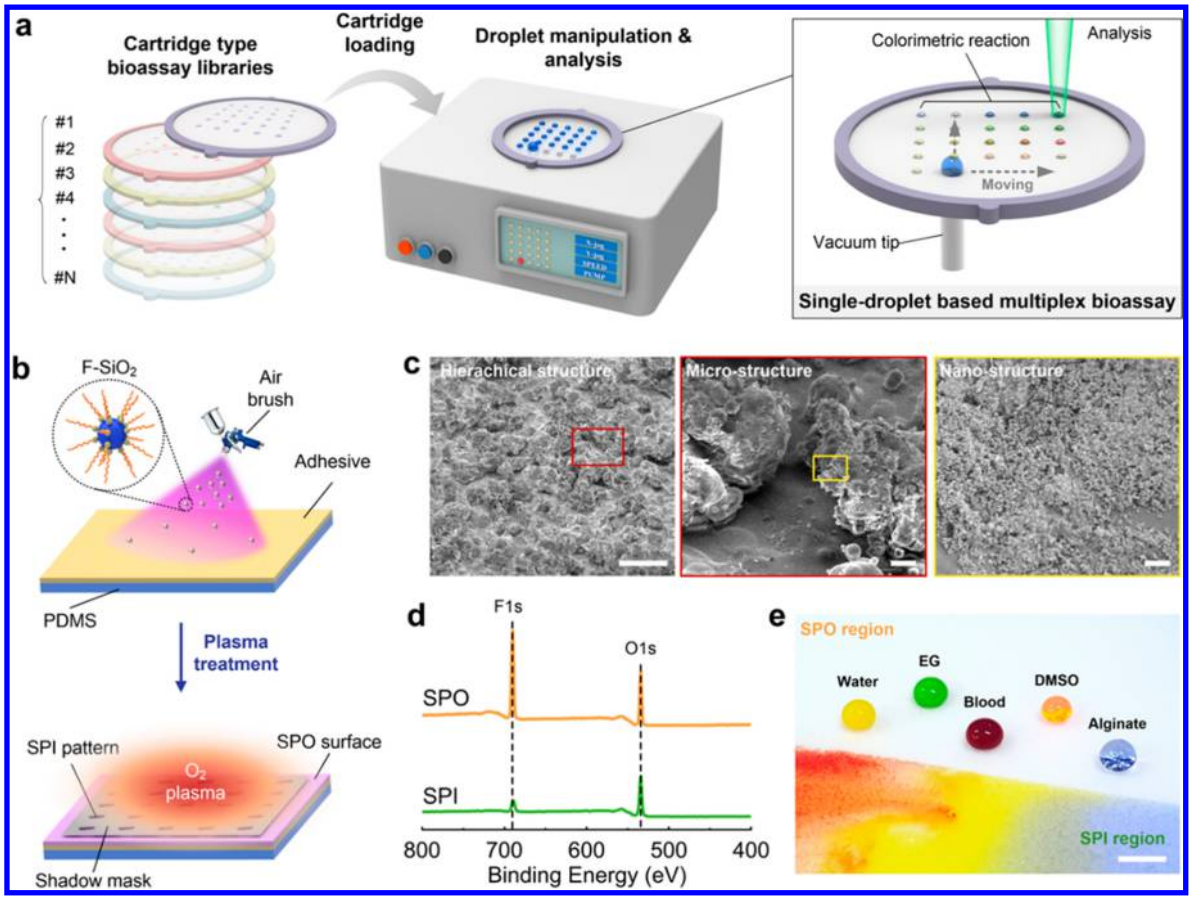

Figure 1. SPO−SPI patterned PDMS substrate for the droplet-based multiplex bioassay platform. (a) Schematic of droplet-based multiplex bioassays on SPO−SPI patterned substrates. A predesigned bioassay library on a disposable cartridge is loaded onto the droplet manipulation platform for single-droplet multiplex bioassays. (b) Schematic of the fabrication process of the SPO−SPI patterned substrate. (c) Scanning electron microscopy images showing the hierarchical micro- and nanostructures of the substrates. Scale bars: 100, 10, and 1 μm for hierarchical-, micro-, and nanostructures, respectively. (d) X-ray photoelectron spectra of the SPO and SPI surfaces. (e) Photograph of various liquids on the SPO and SPI surfaces. Scale bar: 1 cm.

on SPO PDMS while showing a CA of nearly zero on SPI PDMS. In addition to the static CAs, the SAs of each type of sample were measured, and the liquids on the SPO PDMS displayed very low SAs (<10°, Figure S4). The liquid repellency of the prepared substrate was further investigated by measuring the CAs and SAs of various liquid droplets (Figure S5). The droplets with varying surface tensions were prepared by mixing water, which has a high surface tension (72 mN/m) and ethanol, which has a low surface tension (21.8 mN/m) with different mixing ratios. The SPO PDMS substrate showed extreme repellency toward the liquid droplets with a surface tension greater than 33 mN/m, which is lower than that of most biological fluids, such as blood, plasma, sweat, and urine (46−72 mN/m).[37−39] The extreme wettability of the SPO/SPI PDMS substrate can be explained by the low surface energy of the hierarchical micro- and nanostructures. Figure 2d shows a schematic of wettability principles for the hierarchically structured SPO/SPI layers. During the sequential spray-coating process, re-entrant microstructures form from the aerosol of adhesive droplets and agglomerates of F-NPs.[40] Thus, when a liquid with low surface tension is loaded onto the fabricated structures, the meniscus between the liquid and re-entrant cavities adopts a convex shape because of the negative slope of the re-entrant structures and the low surface energy of the F-NPs.[41,42] The gravitational force induced downward intrinsic pressure (P_i) in equilibrium with an upward Laplace pressure (P_L) at the interfaces. In addition, the agglomerated F-NPs contribute to the superamphiphobicity of the substrate by forming a large number of nanoscale pores that contain tiny air pockets (Figure S6).[40,41] Therefore, low-surface-tension liquids and complex biofluids such as EG and blood are excluded from the cavities, resulting in the nonwetting surface with high CA (>150°, Figure 2c). The surface energy drastically increases after the oxygen plasma treatment because it decomposes the low-surface-energy FAS layer.[35] The increased energy of the plasma-treated surface changes the direction of P_L downward, resulting in an almost zero apparent CA of the liquids on the hierarchical structures (Figure S7).[43]

Mechanical Durability of the SPO PDMS Substrate. For the local deformation of surfaces to allow the manipulation of liquid droplets, the extreme wettability of SPO PDMS must be maintained under the stretched state. Figure 3a shows a 10 μL EG droplet on SPO PDMS before and after the application of a uniaxial tensile strain. SPO PDMS retained its liquid repellency at strain levels of as high as 100%. Because of the heterogeneous tensile strain distribution during surface stretching, the micro/nanohierarchical structures were preserved in specific section of the surface (hills), whereas the other sections (valleys) were elongated, exposing the flat PDMS surface (Figure 3b). Thus, the extreme wetting behavior at the macroscopic scale was maintained through the formation of air cavities in partially preserved hierarchical structures, even under

DOI: 10.1021/acsnano.7b05826
ACS Nano XXXX, XXX, XXX−XXX

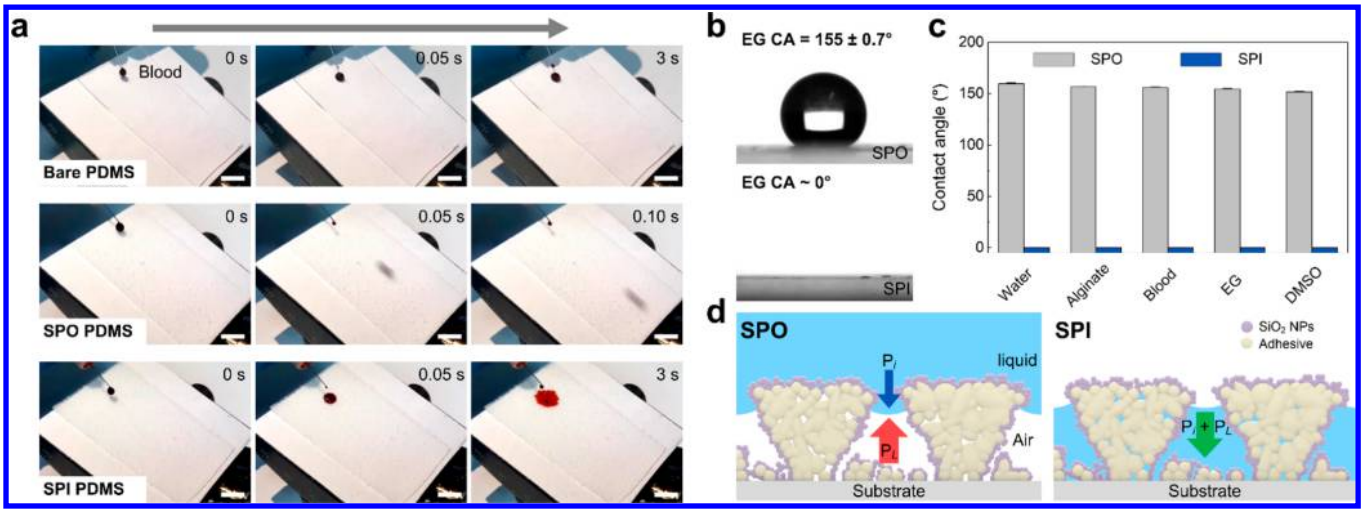

Figure 2. Experimental observations and theoretical principles of the extreme wettability of SPO and SPI PDMS substrates. (a) Sequential photographs of blood droplets on bare, SPO, and SPI PDMS substrates tilted at 20°. Scale bar: 1 cm. (b) Optical images of a 5 μL EG droplet on the SPO and SPI surfaces. (c) CAs of various liquid droplets on the SPO and SPI surfaces. All liquid droplets used in these experiments showed a high CA (>150°) on the SPO surface and an almost zero CA on the SPI surface. d) Schematics of the wettability principles of the SPO and SPI surfaces.

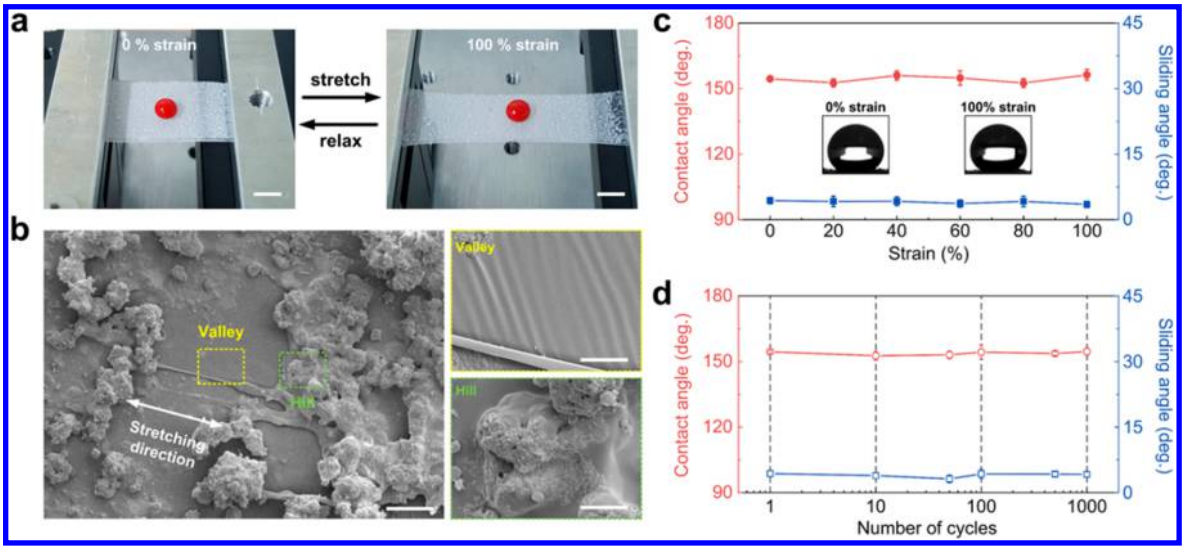

Figure 3. Mechanical durability of the SPO PDMS substrate under repeated stretching cycles. (a) Photographs of the stretching and relaxing of the substrate. Scale bar: 1 cm. (b) SEM images of the substrate under 100% strain. Scale bar: 50 μm. The magnified SEM images indicate that the hierarchical micro- and nanostructures were maintained under stretching. Scale bar: 10 μm. (c,d) CAs and SAs of the EG droplets on the SPO substrate under different uniaxial strains and number of stretching cycles.

100% strain (Figure 3c).[44] In addition, stable adhesion between the coating layer and PDMS substrate contributes to the mechanical durability of SPO PDMS upon repeated stretching (Figure 3d). In these experiments, 100% uniaxial strain is applied and released during each cycle. SPO PDMS showed no defects or delamination of the coating even after 1000 stretch and release cycles (Figure S8), and its initial CA and SA values were unchanged.

Liquid Droplet Manipulation on the SPO–SPI Patterned PDMS Substrate. Using the highly stretchable SPO–SPI patterned PDMS, we demonstrated precise liquid droplet manipulation in the prepared system including transporting, mixing, and dispensing (Figure 4a and Movie S2). The diameter of the circular SPI patterns and the spacing between them were 2 and 15 mm, respectively. A vacuum pressure of 20 kPa was applied beneath the substrate through a 10 mm diameter vacuum tip to load the droplet. Then, the tip was gently pulled down using a *Z*-stage to create a slight slope (~5°). For the manipulation of the liquid, the vacuum tip was horizontally manipulated using an automated *X*–*Y* translation stage. The 200 μL EG droplet freely traveled on the SPO region with the moving vacuum tip and left a few microliters of fluid on the SPI patterns along the path of the vacuum tip. In addition, the manipulation of the blood and multiple other droplets were successfully demonstrated using the fabricated system combined with multiple vacuum tips (Movie S3 and Movie S4). It should be noted that the biofluidic droplet dispensing and multiple droplet guiding are useful in biomedical applications because they enable automated detection and analysis of bioanalytes in a high-throughput manner.

The principle of liquid droplet guiding and dispensing is shown in Figure 4b. Generally, droplet behavior on the surface

DOI: 10.1021/acsnano.7b05826
ACS Nano XXXX, XXX, XXX–XXX

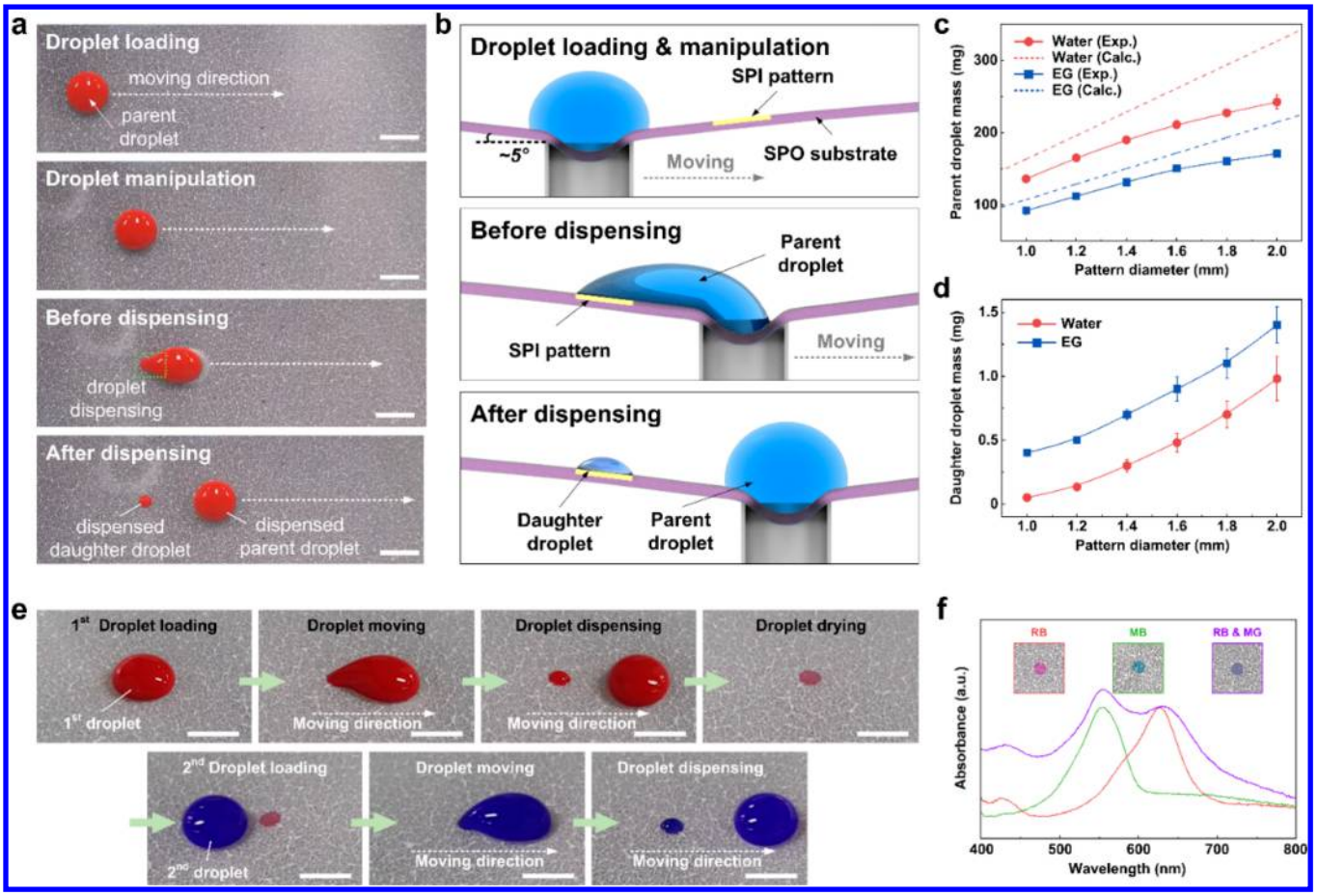

Figure 4. Guiding and dispensing of the liquid droplet on the SPO−SPI patterned PDMS substrate. (a) Sequential photographs of droplet dispensing on the SPO−SPI patterned surface. Scale bar: 1 cm. (b) Schematic diagram showing the principle of droplet guiding and dispensing used in this study. The daughter droplet is dispensed from the parent droplet when the vacuum tip passes the SPI pattern. (c) Mass of the required droplet volume for droplet dispensing as a function of pattern diameter. (d) Mass of the dispensed daughter droplet as a function of pattern diameter. (e) Consecutive photographs of droplet dispensing on a single SPI pattern. The pattern maintains its superamphiphilicity after the first dispensed droplet was dried. Scale bar: 5 mm. (f) Absorption spectra of rhodamine B (RB) and malachite green (MG) on a dyed SPI pattern. The characteristic peaks correspond to the different dyes (RB, 557 nm; MG, 627 nm). After sequential dispensing and drying of the RB and MG dye droplets on a single pattern (denoted as RB and MG) the absorption spectrum shows double peak characteristics, composed of the RB and MG peaks.

is governed by the correlation between the gravity applied to the droplet on a substrate (F_g) and surface adhesion force (F_{adh}). When F_g is larger than F_{adh}, liquid droplets freely move on the substrate with appropriate manipulation. For droplets on a tilted substrate, F_g can be determined by the equation; $F_g = mg \sin \delta$, where m is the mass of the parent droplet, g is the gravitational acceleration, and δ is the tilting angle of the substrate. From the above equation, the adhesion force of the SPO substrate was calculated to be 2.6 mN (Figure S4), which implies that a water droplet greater than ~3 μL can be guided along the local movements of the dimples. Compared to the F_{adh} of SPO substrate, the surface adhesion force of the SPI pattern (F_{SPI}) is extremely high. Thus, when the guided droplet passes the SPI pattern, the droplet sticks to the pattern and is stretched as the vacuum tip moves away from the pattern. The droplet is stretched until F_g becomes equal to F_{SPI}. Then, some of the droplet (daughter droplet) remains from the parent droplet when the tip is moved away from the pattern. In contrast, when F_g is smaller than F_{SPI}, the parent droplet is pinned on the SPI pattern rather than dispensing the daughter droplet. From the Furmidge equation, F_{SPI} can be described by $D\gamma(1 - \cos \theta_{CA})$, where D is the diameter of the pattern, γ is the liquid surface tension, and θ_{CA} is the CA of the droplet on the SPI pattern.[45] Therefore, the conditions required for the droplet to be dispensed onto the SPI pattern can be derived from the following equation:

$$mg \sin \delta \geq D\gamma(1 - \cos \theta_{CA}) \quad (1)$$

Equation 1 implies that the minimum mass of the parent droplet required for droplet dispensing (m_{min}) is in proportion to D and γ. Figure 4c shows the experimentally determined and calculated results of m_{min} as a function of the diameter of the SPI pattern needed to satisfy the droplet dispensing conditions. As predicted from eq 1, the m_{min} increases with SPI pattern diameter. In addition, the m_{min} of the water droplet is clearly larger than that of the EG droplet when using the same SPI pattern. The m_{min} difference between the water and EG droplet can be attributed to the surface tension of water (72.0 mN/m), which is greater than that of EG (47.3 mN/m). The experimentally determined values are smaller than those of the calculation, and the disparity increases as the SPI pattern diameter increases. This behavior can be attributed to the nonuniform adhesion force distribution of the SPI pattern resulting from the deformation of the droplet meniscus.[46] If the volume of the droplet

DOI: 10.1021/acsnano.7b05826
ACS Nano XXXX, XXX, XXX−XXX

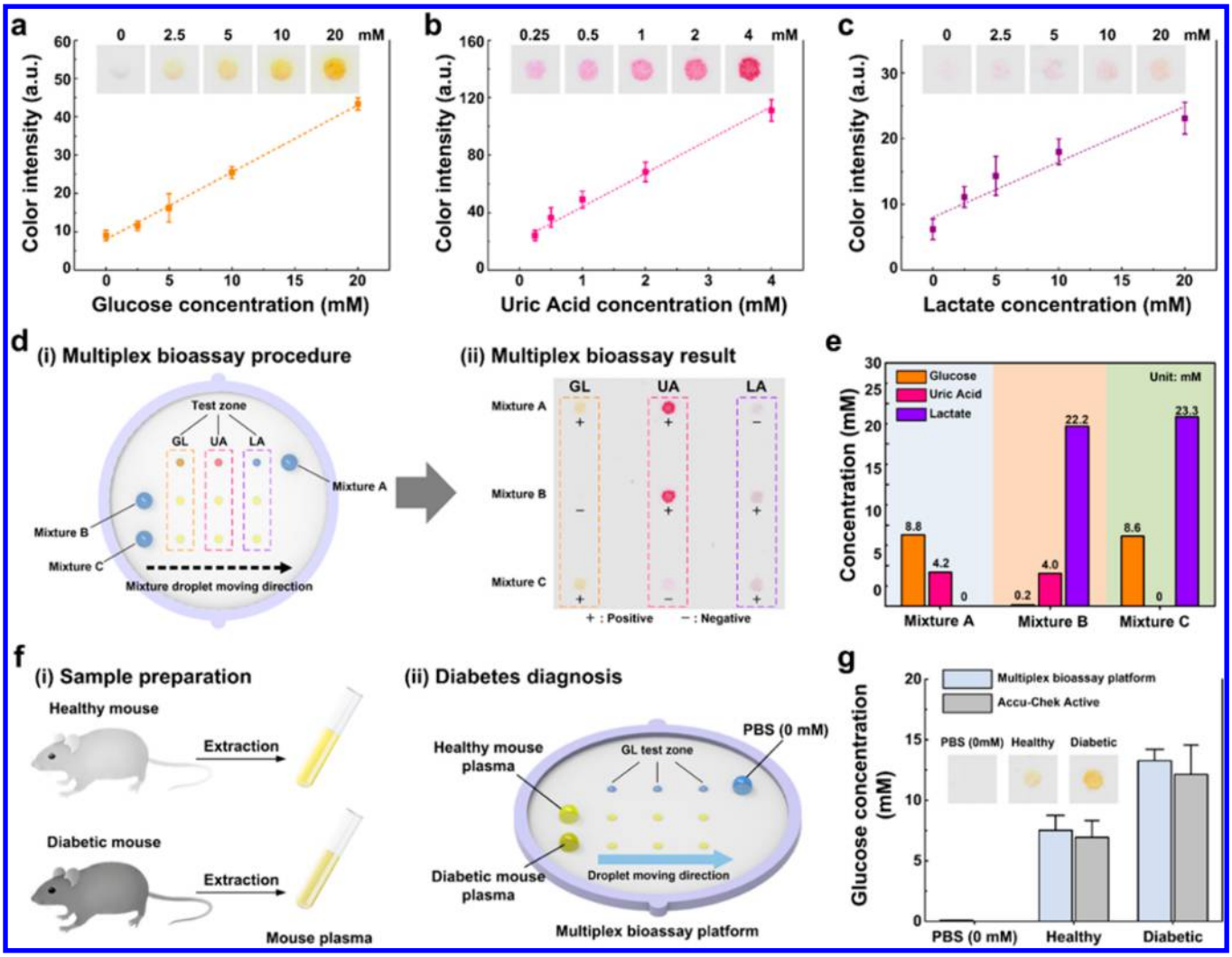

Figure 5. Multiplex colorimetric bioassay and diagnosis of diabetes using the droplet manipulation system. Colorimetric assay results for (a) GL, (b) UA, and (c) LA. The insets show the colorimetric assay images. (d) (i) Schematic of the multiplex bioassay procedure and (ii) colorimetric assay results. The plus (+) and minus (−) signs indicate positive and negative reactions for the colorimetric assay. (e) GL, UA, and LA concentrations determined by the colorimetric results of different mixtures (Mixture A, Mixture B, and Mixture C). (f) Schematics of (i) plasma sample preparation and (ii) the diabetes diagnosis procedure. (g) Comparison of GL concentrations obtained by the colorimetric assay and conventional GL meter (Accu-Check Active). The insets show the colorimetric assay images of pristine PBS (GL, 0 mM), healthy mouse plasma, and diabetic mouse plasma.

increases, the instability of the droplet meniscus shows a similar increase (Figure S9). Thus, the droplet rolls off of the adhesive surface before it can achieve the maximum full pinning force of the SPI pattern. Figure 4d shows the mass of the daughter droplets left on the SPI pattern after dispensing. As can be clearly observed in Figure 4d, a few microliters of the daughter droplet were precisely dispensed, and the mass was determined by diameter of the SPI pattern. When the diameter of the SPI pattern was raised from 1 to 2 mm, small liquid droplets were precisely dispensed with volumes ranging from 0.05 to 1 μL for water and 0.4 to 1.4 μL for EG. Interestingly, the daughter droplet mass of the EG was larger than that of the water at a constant pattern size. This is attributed to the higher surface tension of water than that of EG, resulting in a stronger adhesion to the SPI pattern (eq 1). To determine the limitation of droplet dispensing, SPI patterns with different diameters were fabricated (Figure S10). The results confirmed that water dispensing can be successfully achieved with a pattern diameter as small as 0.6 mm. However, when the diameter is smaller than 0.6 mm, dispensing of the water droplet did not occur since the adhesion force of the SPI region at the smaller diameters was negligible compared to the surface tension of the water droplet.

To apply the developed system as a droplet-based bioassay platform, the extremely high liquid wettability of the SPO−SPI patterns must be maintained. Figure 4e and Movie S5 show the sequential dispensing of two different droplets containing either red or blue dyes on the same 2 mm diameter SPI pattern. Even after dyeing the pattern with the first red droplet, no noticeable change in wettability was observed in the SPI pattern. The blue droplet was successfully dispensed on the red-dyed SPI pattern. Another important consideration is whether the substances in the sample droplets can be sufficiently mixed on the SPI pattern. The mixing of the substances on the SPI pattern was evaluated by sequential staining of the SPI pattern with two different fluorescent dyes Figure 4f shows the absorption spectra of the fluorescent-dye-stained SPO−SPI patterns. First, the absorption spectra of rhodamine B (RB) was measured, and malachite green (MG) was then stained on the

DOI: 10.1021/acsnano.7b05826
ACS Nano XXXX, XXX, XXX−XXX

SPI patterns. The absorption spectra of RB and MG showed significant peaks at 557 and 627 nm, respectively, matching previously reported results.[47,48] Next, the absorption spectrum of an RB/MG mixed pattern formed by successive dyeing and drying of RB and MG on the same SPI pattern was measured. Significantly, the two characteristic peaks appeared at the same wavelengths of the pure RB and MG spectra, suggesting that various specimens can be mixed well and successfully reacted on the SPI pattern. Furthermore, this capability enables colorimetric bioassays where independent colors are extracted from the pattern using a wavelength filter.

Colorimetric Bioassay Using the SPO−SPI Patterned PDMS Substrate-Based Droplet Manipulation System. To determine the analytical efficacy of the developed system, the enzymatic colorimetric assay of three clinical relevant analytes (GL, UA, and LA) were performed using the SPO−SPI patterned PDMS substrate-based droplet manipulation system. For the colorimetric assay, the droplet manipulation system was used to prepattern the SPI regions of the substrate with the colorimetric reagents consisting of enzymes and a color indicator. The droplets containing the biological analytes were then dispensed and fully dried onto the SPI region previously coated with the reagent (see Materials and Methods section for details). Figure 5a−c and the corresponding insets show the results of the colorimetric assay for GL, UA, and LA, respectively. Higher analyte concentrations led to increased color intensity, and linear relationships were obtained over the following concentration ranges: GL (0−20 mM), UA (0.25−4 mM), and LA (0−20 mM). These results are similar to those previously reported for microfluidic paper-based devices.[19,49] The fabricated bioassay substrate exhibited stable wettability and colorimetric response after 2 weeks, regardless of storage conditions (see Figures S11 and S12 and the Supporting Information for more details). It should be noted that the developed system can efficiently reduce sample consumption (1 μL) by reducing handling mistakes and unnecessary waste, such as sample absorption to a microfluidic channel. Furthermore, the developed system enables the simultaneous detection of many analytes in a single run using a single droplet. Figure 5d(i) shows the overall multiplex bioassay procedure. To demonstrate the multiplex bioassay, SPI patterns were formed in a 3 × 3 array on the SPO PDMS substrate, and each of the columns was coated with GL, UA, and LA reagents. Next, three combinations of analyte samples (Table 1) were sequentially dispensed from the top to bottom lines. Figure 5d(ii) shows the multiple analyte detection results for each sample. From the measured color intensity, it was determined that the concentration of each analyte in the sample droplets were similar to the predesigned concentrations within a 20% error, which satisfies the FDA standard (Figure 5e).[50] Compared to conventional microfluidic multiplex bioassays, our system can transfer and pattern the sample droplet without the need for microfluidic channels. Therefore, our system is more suitable for multiplex bioassays as it reduces cross-contamination between reaction zones. To explore the feasibility of the developed system as a practical diagnosis platform, the diabetes state of mice was determined by analyzing the GL concentration in a plasma droplet sample, as shown in Figure 5f. Blood plasma samples were obtained from both healthy and diabetic mice. Figure 5g shows the GL concentrations determined by colorimetric assay. Animals were classified as diabetic if their perfusate GL concentration was higher than 13 mM.[51] The results show that the GL level in the diabetic mouse was 13.3 mM, whereas that in the healthy one was determined to be 7.5 mM. To determine the accuracy of the measured GL concentrations, the samples were also examined using a conventional GL meter (Accu-Check Active), with similar results to those obtained from the colorimetric assay. This implies that our approach can be practically used as a diagnosis platform with high accuracy.

Table 1. Combinations of the Analytes for Testing the Multiplex Colorimetric Bioassays

	glucose (mM)	uric acid (mM)	lactate (mM)
sample 1	10	2	0
sample 2	0	2	2
sample 3	10	0	2

CONCLUSION

Herein, we developed an SPO−SPI patterned PDMS substrate-based droplet manipulation system for multiplex bioassay platforms. The SPO layer was formed by spraying a double layer of adhesive and F-NPs, which is a straightforward and efficient method suitable for spraying of large areas. The SPI region was patterned using an oxygen plasma treatment in combination with a shadow mask. The experimental and theoretical results demonstrated that the SPO and SPI layers exhibited extremely high liquid repellency and adhesive properties toward low surface tension and viscous biofluidic droplets. The extraordinary properties of the SPO−SPI patterned PDMS substrate enabled full-range droplet manipulation, including transportation, mixing, and dispensing, through the control of a local dimple. Based on the developed droplet manipulation system, a multiplex colorimetric bioassay platform was fabricated that is able to precisely determine the concentration of multiple clinically relevant analytes (GL, UA, and LA) using only a single droplet. Furthermore, the feasibility of the developed device as a diagnostic platform was examined by diagnosing diabetes. Therefore, we expect that the developed system will have broad applications in the biomedical field because of its simple fabrication process and potential for easy combination with conventional biosensing methods.

MATERIALS AND METHODS

Preparation of F-NPs. A total of 200 mg of silica nanoparticles (10−20 nm particle size, Sigma-Aldrich) was dispersed in 9.7 g of toluene. Subsequently, 0.1 g of 1*H*,1*H*,2*H*,2*H*-perfluorooctyltriethoxysilane (POTS, Sigma-Aldrich) was added to the silica solution and homogeneously mixed with ultrasonication for 1 h to fluorinate the silica nanoparticles. The solution was then centrifuged (3000 rpm for 30 min) and washed with acetone three times to remove any residual POTS. Finally, the F-NP solution was diluted to 2 wt % in acetone.

Fabrication of the Stretchable SPO PDMS Substrate. A total of 7 g of PDMS (Sylgard 184, Dow Corning) was mixed with a curing agent in a weight ratio of 10:1 and gently poured into a round polystyrene Petri dish (140 mm in diameter) after degassing in a vacuum chamber. The PDMS substrate was cured in an oven at 80 °C for 1 h and carefully peeled off to obtain a ∼340 μm thick PDMS layer. To fabricate the SPO PDMS substrate, 5 g of commercially available bonding material (PART# 4000, Ultra-Ever Dry), composed of acetic acid 1,1-dimethylethyl ester (36 wt %), xylene (36 wt %), acetone (11 wt %), and proprietary polymer material (17 wt %), was spray-coated onto the PDMS substrate using an airbrush (0.5 mm nozzle size, GP-50, Sparmax), followed by drying at 80 °C for 30 min in an oven. The 2 wt % F-NPs solution prepared previously was sprayed onto the bonding-material-coated PDMS substrate using an airbrush

DOI: 10.1021/acsnano.7b05826
ACS Nano XXXX, XXX, XXX−XXX

with the same specifications. The spray-coating processes were conducted under 140 kPa of N_2 pressure at a constant distance of ~20 cm.

Fabrication of SPO–SPI Patterned Substrates. To obtain SPI patterns on the SPO PDMS substrates, the SPO PDMS substrate was plasma treated at 100 W for 45 s (CUTE-MPR, Femto Science) using a patterned shadow mask. The wettability of the region exposed to plasma was changed from SPO to SPI.

Droplet Manipulation on the SPO–SPI Patterned Substrate. For droplet manipulation, the circular SPI regions were patterned in a 2 mm diameter and 15 mm spacing on the SPO PDMS substrate. Then, the SPO–SPI patterned PDMS substrate with a diameter of 140 mm was suspended in a metallic sample stage with an 85 mm diameter central hole without sagging. A vacuum tip (10 mm diameter, 20 kPa of vacuum pressure) was placed beneath the substrate to manipulate the droplet motion. The distance between the substrate and vacuum tip was adjusted using a *Z*-axis stage. The movement of the vacuum tip was precisely controlled by a programmable *X*–*Y* translation stage at a speed of 3 mm/s (see Figure S13 for detailed configuration of the liquid manipulation system).

Investigation of Droplet Dispensing on the SPO–SPI Patterned PDMS Substrate. To study the effect of SPI pattern diameter for droplet dispensing, we prepared various SPO–SPI patterned PDMS substrates by varying the diameter of SPI patterns (1.0, 1.2, 1.4, 1.6, 1.8, and 2.0 mm). The substrate was then placed on a digital scale with tilting angle of 5°. To measure the minimum dispensable volume from the parent droplet, successive microdrops were placed on the patterns using an insulin syringe (BD Ultra-Fine II) until the droplet was completely dispensed. The mass of the daughter droplet was then measured using a similar procedure.

Investigation of Droplet Patterning Using a Fluorescent Dye. RB and MG were purchased from Sigma-Aldrich and were dissolved in DI water to a final concentration of 0.1 mM. The absorption spectra of RB, MG, and mixed RB/MG were measured using a UV–vis spectrophotometer (V-650, JASCO).

Colorimetric-Analysis-Based Multiplex Bioassays. The D-(+)-GL (99%), UA (99%), LA (99%), glucose oxidase (GOx, from *Aspergillus niger*, 128200 U/g), uricase (UC, from *Candida* sp., 5 U/mg), lactate oxidase (LOx, from *Pediococcus* sp., 20 U/mg), peroxidase (HRP, from horseradish, 146 U/mg), D-(+)-trehalose dehydrate (TRH, 98.5%), 4-aminoantipyrine (4-AAP, reagent grade), 3,5-dichloro-2-hydroxybenzenesulfonate (DHBS, 98%), and *o*-dianisidine dihydrochloride (OD, 95%) were purchased from Sigma-Aldrich. Potassium iodide (KI, 99.5%) was purchased from Duksan Chemical. All colorimetric reagents were prepared by mixing the enzyme and chromogenic solutions in a 1:1 ratio. For the glucose assay, the enzyme solution was prepared by dissolving GOx (100 U/mL), HRP (30 U/mL), and TRH (0.3 M) in 100 mM PBS (pH 6.0). The chromogenic reagent was prepared by dissolving KI in 100 mM PBS (pH 6.0) to a final concentration of 0.6 M. For the uric acid assay, the enzyme solution was prepared by dissolving UC (80 U/mL), HRP (300 U/mL), and TRH (0.3 M) in 100 mM PBS (pH 6.0). For this solution, the chromogenic reagent was prepared by dissolving 4-AAP (4 mM) and DHBS (8 mM) in 100 mM PBS (pH 6.0). For the lactate assay, the enzyme solution was prepared by dissolving LOx (10 U/mL), HRP (30 U/mL), and TRH (0.3 M) in 100 mM PBS (pH 6.0). The OD was dissolved in 100 mM PBS (pH 6.0) to a final concentration of 31 mM and acted as the chromogenic reagent. Analytes including GL (0, 2.5, 5, 10, and 20 mM), UA (0.25, 0.5, 1, 2, and 4 mM), and LA (0, 2.5, 5, 10, and 20 mM) were prepared in various concentrations. To prepare the analytical zone, 1 μL of colorimetric reagents containing the selected enzyme and chromogenic solutions was dispensed in the 2 mm diameter circular SPI regions using the droplet manipulation system and were fully dried at room temperature for 30 min. Then, 1 μL of solutions containing the analytes was dispensed onto the colorimetric reagent prepatterned SPI regions and dried at room temperature for 30 min. The timed needed for evaporation of the liquid dispensed in 2 mm diameter SPI pattern exceeded 30 min, providing a sufficient time for the colorimetric assay response (Figure S14). In addition, loss of the sample during the guiding and dispensing of the droplet by evaporation was negligible and did not affect the colorimetric assay results (Figure S15). A scanner was used to acquire images of the colorimetric detection on the SPO–SPI patterned substrates and the color intensity of the images was analyzed using the Adobe Photoshop CS6 software. For diabetes diagnosis, mouse sera were acquired from healthy and diabetic mice[52] (ICR, 7-week old, female; purchased from Orientbio Seongnam, Gyeonggi, Korea). A glucometer (ACCU-CHEK Active, Roche, Basel, Switzerland) was used to compare the results of the developed multiplex assay platform.

Characterization. The surface morphologies of the SPO–SPI patterned PDMS substrate were characterized using a field-emission scanning electron microscope (JSM-6360, JEOL). The chemical composition of the substrate was determined using an X-ray photoelectron spectrometer (K-alpha, Thermo Scientific) equipped with a monochromatic Al Kα X-ray source. The static CAs of the liquids were measured using a CA measurement system equipped with a dynamic image capture camera (Phoenix 300, SEO Co., Ltd.). In this study, the SAs were defined as the tilting angle when the droplet began to move across the surface. To measure the SAs, 10 μL of liquid droplets were placed on the substrate, and the tilting angle was gently increased using a manual tilting stage until the droplet rolled off.

ASSOCIATED CONTENT

Supporting Information

The Supporting Information is available free of charge on the ACS Publications website at DOI: 10.1021/acsnano.7b05826.

Photographs of the SPO layer coatings on various materials; examples of the SPO–SPI patterned PDMS substrate; SEM images of SPO layer before and after oxygen plasma treatment; sliding angles of liquid droplets on the SPO surfaces; CAs and SAs of the various liquid droplets on the SPO-layer-coated substrate with different surface tensions; SEM images of the spray coated layer with only adhesive or F-NPs; photographs of the SiO_2 substrates with different surface conditions; SEM images of SPO PDMS substrate after 1000 cycles of stretching with 100% strain; photographs showing the instability of the droplet meniscus; optical image of a circularly patterned shadow mask and the resulting SPO–SPI patterned PDMS substrate; wetting stability of the coatings over time; colorimetric response stability of the developed bioassay platform over time; photograph of the configuration of the developed system; experimentally determined and theoretically calculated evaporation time of the dispensed droplets on patterns with various diameters; mass loss of the water droplet on the SPO PDMS substrate (PDF)

Movie S1: Extreme wettability of the SPO and SPI PDMS substrates (AVI)

Movie S2: Droplet manipulation including transporting, mixing, and dispensing (AVI)

Movie S3: Manipulation of a viscous heparinized blood droplet (AVI)

Movie S4: Multiple droplet guiding (AVI)

Movie S5: Stable wettability of the SPO–SPI patterned substrate after dyeing (AVI)

AUTHOR INFORMATION

Corresponding Authors

*E-mail: jungmokseo@kist.re.kr.

*E-mail: taeyoon.lee@yonsei.ac.kr.

ORCID

Seung-Woo Cho: 0000-0001-8058-332X

Taeyoon Lee: 0000-0002-8269-0257

DOI: 10.1021/acsnano.7b05826
ACS Nano XXXX, XXX, XXX–XXX

Author Contributions

H.H. conducted the experiments, measurements, and analysis and wrote the manuscript. J.S.L. provided assistance for the bioassay experiments. H.K. fabricated the SPO PDMS substrate, S.S. supported the graphical works of the figures. J.K. designed the fabrication method of the SPO substrate. J.L., X.H., and S.W.C. provided helpful discussions regarding data analysis. J.S. conceived of and designed the study and revised the manuscript. T.L. and J. S. supervised the project.

Notes

The authors declare no competing financial interest.

ACKNOWLEDGMENTS

This work was supported by the Priority Research Centers Program (2012-0006689) through the National Research Foundation (NRF) of Korea funded by the Ministry of Education, Science and Technology (MEST), and the R&D program of MOTIE/KEIT [10064081, Development of fiber-based flexible multimodal pressure sensor and algorithm for gesture/posture-recognizable wearable devices]. We gratefully acknowledge partial support from the National Research Foundation of Korea (NRF-2017K2A9A2A06013377 and NRF-2017M3A7B4049466). This work is also supported by KIST project (2E27930). This study was supported by the Bio & Medical Technology Development Program of the NRF funded by the Korean government MSIP (2015M3A9E2029265). This work was also supported by the Recruitment Program for Young Professionals (China), the National Natural Science Foundation (China, 21673197).

REFERENCES

(1) Wang, G.; Ho, H.-P.; Chen, Q.; Yang, A. K.-L.; Kwok, H.-C.; Wu, S.-Y.; Kong, S.-K.; Kwan, Y.-W.; Zhang, X. A Lab-in-a-Droplet Bioassay Strategy for Centrifugal Microfluidics with Density Difference Pumping, Power to Disc and Bidirectional Flow Control. *Lab Chip* **2013**, *13*, 3698−3706.

(2) Popova, A. A.; Schillo, S. M.; Demir, K.; Ueda, E.; Nesterov-Mueller, A.; Levkin, P. A. Droplet-Array (DA) Sandwich Chip: A Versatile Platform for High-Throughput Cell Screening Based on Superhydrophobic-Superhydrophilic Micropatterning. *Adv. Mater.* **2015**, *27*, 5217−5222.

(3) Shin, S.; Seo, J.; Han, H.; Kang, S.; Kim, H.; Lee, T. Bio-Inspired Extreme Wetting Surfaces for Biomedical Applications. *Materials* **2016**, *9*, 116−141.

(4) Hou, X.; Zhang, Y. S.; Santiago, G. T.; Alvarez, M. M.; Ribas, J.; Jonas, S. J.; Weiss, P. S.; Andrews, A. M.; Aizenberg, J.; Khademhosseini, A. Interplay between Materials and Microfluidics. *Nat. Rev. Mater.* **2017**, *2*, 17016−17030.

(5) Hernández, S. C.; Bennett, C. J. C.; Junkermeier, C. E.; Tsoi, S. D.; Bezares, F. J.; Stine, R.; Robinson, J. T.; Lock, E. H.; Boris, D. R.; Pate, B. D.; Caldwell, J. D.; Reinecke, T. L.; Sheehan, P. E.; Walton, S. G. Chemical Gradients on Graphene to Drive Droplet Motion. *ACS Nano* **2013**, *7*, 4746−4755.

(6) Pollack, M. G.; Fair, R. B.; Shenderov, A. D. Electrowetting-Based Actuation of Liquid Droplets for Microfluidic Applications. *Appl. Phys. Lett.* **2000**, *77*, 1725−1726.

(7) Lee, S.; Lee, S.; Kim, D.; Seo, J.; Mahata, C.; Hwang, H.; Algadi, H.; Al-Sayari, S.; Chae, Y.; Lee, T. Electrostatically-Induced Trajectory Switching System on a Multi-Inlet-Multi-Outlet Superhydrophobic Droplet Guiding Track. *RSC Adv.* **2015**, *5*, 5754−5761.

(8) Lee, S.; Lee, S.; Hwang, H.; Hong, J.; Lee, S.; Lee, J.; Chae, Y.; Lee, T. Ultrafast Single-Droplet Bouncing Actuator with Electrostatic Force on Superhydrophobic Electrodes. *RSC Adv.* **2016**, *6*, 66729−66737.

(9) Zhang, Y.; Wang, T. H. Full-Range Magnetic Manipulation of Droplets *via* Surface Energy Traps Enables Complex Bioassays. *Adv. Mater.* **2013**, *25*, 2903−2908.

(10) Zhu, Y.; Antao, D. S.; Xiao, R.; Wang, E. N. Real-Time Manipulation with Magnetically Tunable Structures. *Adv. Mater.* **2014**, *26*, 6442−6446.

(11) Park, S.-Y.; Kalim, S.; Callahan, C.; Teitell, M. a; Chiou, E. P. Y. A Light-Induced Dielectrophoretic Droplet Manipulation Platform. *Lab Chip* **2009**, *9*, 3228−3235.

(12) Chiou, P. Y.; Ohta, A. T.; Wu, M. C. Massively Parallel Manipulation of Single Cells and Microparticles Using Optical Images. *Nature* **2005**, *436*, 370−372.

(13) Guttenberg, Z.; Muller, H.; Habermüller, H.; Geisbauer, A.; Pipper, J.; Felbel, J.; Kielpinski, M.; Scriba, J.; Wixforth, A. Planar Chip Device for PCR and Hybridization with Surface Acoustic Wave Pump. *Lab Chip* **2005**, *5*, 308−317.

(14) McHale, G.; Newton, M. I. Liquid Marbles: Topical Context within Soft Matter and Recent Progress. *Soft Matter* **2015**, *11*, 2530−2546.

(15) Seo, J.; Lee, S.; Lee, J.; Lee, T. Guided Transport of Water Droplets on Superhydrophobic− Hydrophilic Patterned Si Nanowires. *ACS Appl. Mater. Interfaces* **2011**, *3*, 4722−4729.

(16) You, I.; Lee, T. G.; Nam, Y. S.; Lee, H. Fabrication of a Micro-omnifluidic Device by Omniphilic/Omniphobic Patterning on Nano-structured Surfaces. *ACS Nano* **2014**, *8*, 9016−9024.

(17) Seo, J.; Lee, S.; Han, H.; Jung, H. B.; Hong, J.; Song, G.; Cho, S. M.; Park, C.; Lee, W.; Lee, T. Gas-Driven Ultrafast Reversible Switching of Super-Hydrophobic Adhesion on Palladium-Coated Silicon Nanowires. *Adv. Mater.* **2013**, *25*, 4139−4144.

(18) Seo, J.; Lee, S. K.; Lee, J.; Lee, J. S.; Kwon, H.; Cho, S. W.; Ahn, J. H.; Lee, T. Path-Programmable Water Droplet Manipulations on an Adhesion Controlled Superhydrophobic Surface. *Sci. Rep.* **2015**, *5*, 12326−12335.

(19) Martinez, A. W.; Phillips, S. T.; Butte, M. J.; Whitesides, G. M. Patterned Paper as a Platform for Inexpensive, Low-Volume, Portable Bioassays. *Angew. Chem., Int. Ed.* **2007**, *46*, 1318−1320.

(20) Kuan, C.-M.; York, R. L.; Cheng, C.-M. Lignocellulose-Based Analytical Devices: Bamboo as an Analytical Platform for Chemical Detection. *Sci. Rep.* **2016**, *5*, 18570−18580.

(21) Rice, D.; Kocurek, B.; Snead, C. A. Chronic Disease Management for Diabetes: Baylor Health Care System's Coordinated Efforts and the Opening of the Diabetes Health and Wellness Institute. *Proc. (Bayl. Univ. Med. Cent).* **2010**, *23*, 230−234.

(22) Liu, T.; Liu, B.; Zhang, H.; Wang, Y. The Fluorescence Bioassay Platforms on Quantum Dots Nanoparticles. *J. Fluoresc.* **2005**, *15*, 729−733.

(23) Li, H.; Qiang, W.; Wang, C.; Vuki, M.; Xu, D. Ultrasensitive and Fast Fluorescent Bioassay Based on Fluorescence Enhancement of Silver Nanoparticles. *Analyst* **2013**, *138*, 7376−7383.

(24) Wang, J. Electrochemical Glucose Biosensors. *Chem. Rev.* **2008**, *108*, 814−825.

(25) Grieshaber, D.; Mackenzie, R.; Vörös, J.; Reimhult, E. Electrochemical Biosensors -Sensor Principles and Architectures. *Sensors* **2008**, *8*, 1400−1458.

(26) Liu, X.; Dong, M.; Qi, H.; Gao, Q.; Zhang, C. Electrogenerated Chemiluminescence Bioassay of Two Protein Kinases Incorporating Peptide Phosphorylation and Versatile Probe. *Anal. Chem.* **2016**, *88*, 8720−8727.

(27) Zhao, L.; Sun, L.; Chu, X. Chemiluminescence Immunoassay. *TrAC, Trends Anal. Chem.* **2009**, *28*, 404−415.

(28) Hill, H. D.; Mirkin, C. A. The Bio-Barcode Assay for the Detection of Protein and Nucleic Acid Targets Using DTT-Induced Ligand Exchange. *Nat. Protoc.* **2006**, *1*, 324−336.

(29) Yin, H.-q.; Jia, M.-x.; Yang, S.; Wang, S. qi; Zhang, J.-g. A Nanoparticle-Based Bio-Barcode Assay for Ultrasensitive Detection of Ricin Toxin. *Toxicon* **2012**, *59*, 12−16.

(30) Li, W.; Li, J.; Qiang, W. B.; Xu, J. J.; Xu, D. K. Enzyme-Free Colorimetric Bioassay Based on Gold Nanoparticle-Catalyzed Dye Decolorization. *Analyst* **2013**, *138*, 760−766.

DOI: 10.1021/acsnano.7b05826
ACS Nano XXXX, XXX, XXX−XXX

(31) Lim, K. R.; Park, J. M.; Choi, H. N.; Lee, W. Y. Gold Glyconanoparticle-Based Colorimetric Bioassay for the Determination of Glucose in Human Serum. *Microchem. J.* **2013**, *106*, 154−159.
(32) Martinez, A. W.; Phillips, S. T.; Whitesides, G. M.; Carrilho, E. Diagnostics for the Developing World: Microfluidic Paper-Based Analytical Devices. *Anal. Chem.* **2010**, *82*, 3−10.
(33) Gonzalez, A.; Estala, L.; Gaines, M.; Gomez, F. A. Mixed Thread/paper-Based Microfluidic Chips as a Platform for Glucose Assays. *Electrophoresis* **2016**, *37*, 1685−1690.
(34) Wu, P.; Zhang, C. Low-Cost, High-Throughput Fabrication of Cloth-Based Microfluidic Devices Using a Photolithographical Patterning Technique. *Lab Chip* **2015**, *15*, 1598−1608.
(35) Li, Y.; Li, L.; Sun, J. Bioinspired Self-Healing Superhydrophobic Coatings. *Angew. Chem., Int. Ed.* **2010**, *49*, 6129−6133.
(36) Leslie, D. C.; Waterhouse, A.; Berthet, J. B.; Valentin, T. M.; Watters, A. L.; Jain, A.; Kim, P.; Hatton, B. D.; Nedder, A.; Donovan, K.; Super, E. H.; Howell, C.; Johnson, C. P.; Vu, T. L.; Bolgen, D. E.; Rifai, S.; Hansen, A. R.; Aizenberg, M.; Super, M.; Aizenberg, J.; et al. A Bioinspired Omniphobic Surface Coating on Medical Devices Prevents Thrombosis and Biofouling. *Nat. Biotechnol.* **2014**, *32*, 1134−1140.
(37) Harkins, H. N.; Harkins, W. D. The Surface Tension of Blood Serum, and the Determination of the Surface Tension of Biological Fluids. *J. Clin. Invest.* **1929**, *7*, 263−281.
(38) Randall, W. C.; Calman, C. The Surface Tension of Human Sweat; Its Determination and Its Significance. *J. Invest. Dermatol.* **1954**, *23*, 113−118.
(39) Perryman, P. W.; Selous, C. F. Some Physiological and Physical Aspects of the Surface Tension of Urine. *J. Physiol.* **1935**, *85*, 128−144.
(40) Neelakantan, N. K.; Weisensee, P. B.; Overcash, J. W.; Torrealba, E. J.; King, W. P.; Suslick, K. S. Spray-on Omniphobic ZnO Coatings. *RSC Adv.* **2015**, *5*, 69243−69250.
(41) Kim, D.; Seo, J.; Shin, S.; Lee, S.; Lee, K.; Cho, H.; Shim, W.; Lee, H. B. R.; Lee, T. Reversible Liquid Adhesion Switching of Superamphiphobic Pd-Decorated Ag Dendrites *via* Gas-Induced Structural Changes. *Chem. Mater.* **2015**, *27*, 4964−4971.
(42) Weisensee, P. B.; Torrealba, E. J.; Raleigh, M.; Jacobi, A. M.; King, W. P. Hydrophobic and Oleophobic Re-Entrant Steel Microstructures Fabricated Using Micro Electrical Discharge Machining. *J. Micromech. Microeng.* **2014**, *24*, 095020.
(43) Tian, Y.; Jiang, L. Wetting, Intrinsically Robust Hydrophobicity. *Nat. Mater.* **2013**, *12*, 291−292.
(44) Lee, W. K.; Jung, W. B.; Nagel, S. R.; Odom, T. W. Stretchable Superhydrophobicity from Monolithic, Three-Dimensional Hierarchical Wrinkles. *Nano Lett.* **2016**, *16*, 3774−3779.
(45) Furmidge, C. G. L. The Sliding of Liquid Drops on Solid Surfaces and a Theory for Spray Retentioin. *J. Colloid Sci.* **1962**, *17*, 309−324.
(46) Dorrer, C.; Rühe, J. Mimicking the Stenocara Beetle - Dewetting of Drops from a Patterned Superhydrophobic Surface. *Langmuir* **2008**, *24*, 6154−6158.
(47) Kristoffersen, A. S.; Erga, S. R.; Hamre, B.; Frette, Ø. Testing Fluorescence Lifetime Standards Using Two-Photon Excitation and Time-Domain Instrumentation: Rhodamine B, Coumarin 6 and Lucifer Yellow. *J. Fluoresc.* **2014**, *24*, 1015−1024.
(48) Rengifo-Herrera, J. A.; Pizzio, L. R.; Blanco, M. N.; Roussel, C.; Pulgarin, C. Photocatalytic Discoloration of Aqueous Malachite Green Solutions by UV-Illuminated TiO_2 Nanoparticles under Air and Nitrogen Atmospheres: Effects of Counter-Ions and pH. *Photochem. Photobiol. Sci.* **2011**, *10*, 29−34.
(49) Dungchai, W.; Chailapakul, O.; Henry, C. S. Use of Multiple Colorimetric Indicators for Paper-Based Microfluidic Devices. *Anal. Chim. Acta* **2010**, *674*, 227−233.
(50) Freckmann, G.; Schmid, C.; Baumstark, A.; Rutschmann, M.; Haug, C.; Heinemann, L. Analytical Performance Requirements for Systems for Self-Monitoring of Blood Glucose With Focus on System Accuracy. *J. Diabetes Sci. Technol.* **2015**, *9*, 885−894.
(51) Yu, X.; Tesiram, Y. A.; Towner, R. A.; Abbott, A.; Patterson, E.; Huang, S.; Garrett, M. W.; Chandrasekaran, S.; Matsuzaki, S.; Szweda, L. I.; Gordon, B. E.; Kem, D. C. Early Myocardial Dysfunction in Streptozotocin-Induced Diabetic Mice: A Study Using *in Vivo* Magnetic Resonance Imaging (MRI). *Cardiovasc. Diabetol.* **2007**, *6*, 6−13.
(52) Park, J. H.; Kim, S.; Hong, H. S.; Son, Y. Substance P Promotes Diabetic Wound Healing by Modulating Inflammation and Restoring Cellular Activity of Mesenchymal Stem Cells. *Wound Repair Regen.* **2016**, *24*, 337−348.

DOI: 10.1021/acsnano.7b05826
ACS Nano XXXX, XXX, XXX−XXX